ISSN 1023-1935, Russian Journal of Electrochemistry, 2012, Vol. 48, No. 4, pp. 434–441. © Pleiades Publishing, Ltd., 2012.
Published in Russian in Elektrokhimiya, 2012, Vol. 48, No. 4, pp. 478–486.

Ionic Liquids: Electrochemical Investigation on Corrosion Activity of Ethyl-Dimethyl-Propylammonium Bis(Trifluoromethylsulfonyl)Imide at High Temperature[1, 2]

I. Perissi[a, b, z], U. Bardi[a, b], S. Caporali[a, b], A. Fossati[a, b], A. Lavacchi[c], and F. Vizza[c]

[a] *Dipartimento di Chimica, Università di Firenze, Via della Lastruccia, 3–50019 Sesto Fiorentino (FI) Italy*
[b] *Consorzio Interuniversitario Nazionale di Scienza e Tecnologia dei Materiali (INSTM), Unita di Ricerca di Firenze, 50147 Firenze, Italy*
[c] *Istituto di Chimica dei Composti Organometallici (ICCOM-CNR), Via Madonna del Piano 10, 50019, Sesto Fiorentino (FI), Italy*

Received April 20, 2011

Abstract—In the present work we report on our investigation on the corrosion properties of the ethyl-dimethyl-propylammonium bis(trifluoromethylsulphonyl)imide at temperatures up to 473 K. The tests were performed both for commercially pure iron alloys and for pure copper. The electrochemical measurements showed that the metals corrosion rates can be dramatically reduced by purging the ionic liquid with inert gases to remove the dissolved oxygen.

Keywords: ionic liquids, corrosion science, diathermic fluid, electrochemical impedance spectroscopy
DOI: 10.1134/S1023193512030093

INTRODUCTION

In the recent times the Ionic Liquids (ILs) have been exploited for a wide variety of technological applications due to there environmentally benign nature [1–3]. Among the most promising there are lubrication, heat exchange, energy storage, biotechnology, nanotechnology, electrodeposition and fine and bulk chemical synthesis [4–13]. Despite to this exceptionally large potential only a little is known about the thermal stability on the timescale of days and more of the ILs. The literature mainly reports ILs decomposition temperature data derived from Differential Scanning Calorimetry (DSC) or Thermogravimetry (TGA) experiments, where only the short time stability is evaluated. Further the experiments are performed under inert atmosphere and using inert materials for the pans such as alumina. Recent studies demonstrated that such data can only provide a rough estimation of the stability of the ILs, while for a reliable technological assessment other tests are required [14, 15].

According to the high temperature immersion tests in the ILs of a variety of metals and alloys for times up to 40 days we found that the tetra alkyl ammonium cation based ILs are, in principle, sufficiently stable for practical application [16], in a previous investigation [11], we showed also that the quaternary ammonium salt ethyl-dimethyl-propylammonium bis(trifluoromethylsulphonyl) EdMPNTf_2N, is in examples a potential candidate for substituting the conventional diathermic oils in the heat exchange processes.

But this is not the whole story. Having a stable ionic liquid does not mean that it can be used in practice. The interaction of the IL with the materials may also lead to problems. Mainly we may notice that the ILs are electrolytes with a strong attitude to dissolve electro active species such as oxygen and water [17–20]. This is a potentially dangerous combination, especially for the metals, as it provide a suitable environment for corrosion. Only a few investigations have been reported so far on the corrosion of metals and alloys in the Ionic Liquids while, we believe, this is one of the major issues for the technological application. Such a lack of knowledge calls for corrosion science investigations aimed at screening the IL/material combinations for the selection of the systems and also leading to design criteria (sealing, purging, etc.). Even from the point of view of the fundamental investigation the subject is plenty of opportunities as the interpretation of the phenomena occurring at the metal/IL interface is a challenging topic still far from a satisfactory understanding.

In the present paper we report a corrosion science investigation of several metals and alloys (AISI 1018 carbon steel, AISI 304 stainless steel and copper) in EdMPNTf_2N. The materials were selected for their

[1] Published on the basis of the materials of the IXth International Frumkin Symposium "Materials and Technologies of Electrochemistry of the XXIst Century" (Moscow, October, 2010).
[2] The article is published in the original.
[z] Corresponding author: ilaria.perissi@inifi.it (I. Perissi).

application in the field of thermal exchange in solar trough collectors where, as mentioned before, the ILs are potential candidate as *Diathermic fluids*. The investigations are mainly oriented at estimating the entity of the corrosion processes as a function of the materials and the environment. For a more fundamental investigation aimed the understanding of the mechanisms investigation are still in progress and we defer them to future works.

EXPERIMENTAL

The corrosion study of EdMPNTf$_2$N (T_{dec} 593 K, viscosity 71.63 mm^2 s^{-1} at 293 K, water <10000 ppm, Merck KGaA) has been conducted in a customized pressure vessel combined with a small volume Teflon cell. Both the cell and the vessel were realized according by designs developed in our laboratory.

The pressure vessel is a not stirred reactor (PA N4601CH, 1000 mL) from Parr-Instrument Company. The reactor was modified by Parr to allocate a typical three electrodes arrangement. Also a dip tube to inlet the gas and a thermocouple were added to the vessel. The reactor head and body, the thermowell, the dip tube and the three electrodes (insulated from the head by PTFE) are made in Hastelloy C-276; the external gages and the manometer (0–2000 psi) are in stainless steel T316. The modified vessel was tested at 623 K up to 130 bar. The vessel heater consists in a CalRod® mantle, equipped by a control unit to generate temperature ramps.

Inside the pressure vessel was allocated a Teflon® electrochemical cell, designed to guarantee reproducible reciprocal distances among the three electrodes. The cell was realized in our laboratory using a Teflon® bar specifically shaped to hold the working electrode (WE) disk, the thermowell, the gas inlet dip tube, the counter (CE) and the reference (RE) electrodes. The cell has been rigidly fixed to the vessel head using two brass bars. Detailed view of the cell is shown in Fig. 1.

The electrochemical investigation has been carried out using a Potentiostat/Galvanostat PARSTATS 2273, Ametek Inc. The counter-electrodes and reference electrodes were constituted by platinum wires (99.9%, Goodfellow).

Copper (purity 99.99+%, density 8.96 g cm^{-3}, Goodfellow), AISI 1018 carbon steel, (0.14–0.20 wt % C, 0.60–0.90 wt % Mn, 0.035 wt % P, 0.040 wt % S, density 7.87 g cm^{-3}, McMaster-Carr) and AISI 304 stainless steel (Cr 17–20%, Mn <2%, Ni 8–11%, C <80%, density 7.93 g cm^{-3} from Goodfellow) bars were used to prepare WE as thin disks (thickness < 0.5 mm). The disk surface was grinded with SiC paper down to 1200 grit, in order to achieve a reproducible finishing. The geometric area exposed to the IL was 50 mm^2 and the sample was placed as close as possible (<1 mm) to the RE, in order to minimize the ohmic drop. The same refinement was made for a Pt disk, used as WE to test the Pt wire stability respect to the Ferrocene (purum > 98%, mp 445–447 K, Fluka)/Ferrocenium redox couple.

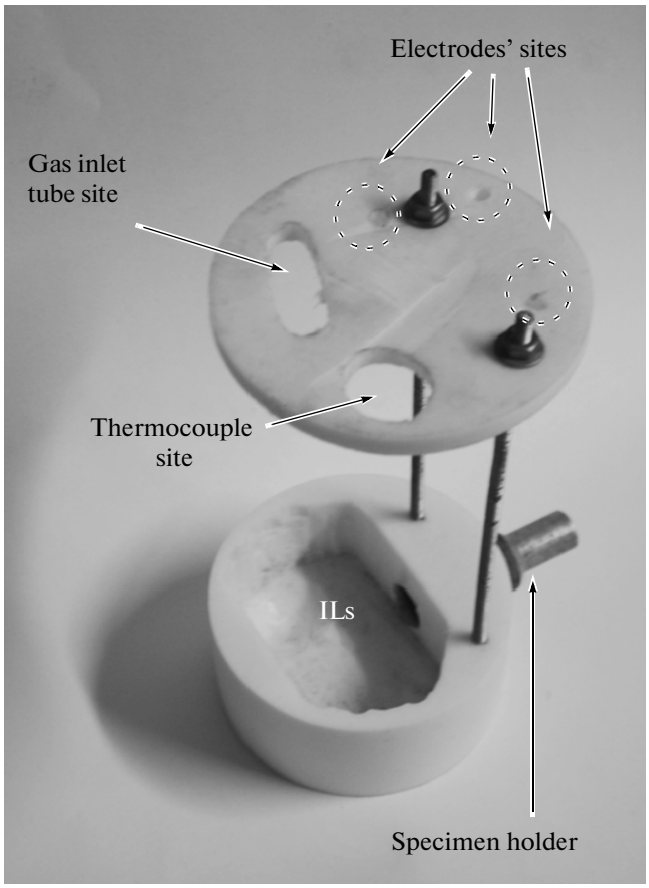

Fig. 1. Image of the reaction cell.

RESULT AND DISCUSSION

Liquid Purging with N_2

An important topic is constituted by the time required to purge the liquid from oxygen/air before the experiments. we have considered purging the liquid bubbling nitrogen. The estimated time of purging was calculated considering the oxygen removing from the solution only due to diffusion. This condition gives an overestimated time of purging respect to a bubbling process, in which also convection process concurs to the oxygen removal.

In the diffusion equation:

$$\frac{dc}{dt} = D_{O_2}\frac{\partial^2 c}{\partial x^2}, \quad (1)$$

where D_{O_2} is the diffusion coefficient of oxygen in the IL, c the initial O_2 concentration, x is the coordinate laying the IL solution depth, and, as initial condition, c is taken as due to the equilibrium with atmospheric oxygen and it is around 7×10^{-4} mol dm^{-3} or 22.4 mg dm^{-3}.

Table 1. CVs data for the Ferrocene/Ferrocenium redox couple (5 mM) at several temperatures ranging from 298 up to 423 K

V_{scan}, mV s^{-1}	T, K	$-Ip_c$, A cm^{-2}	Ip_a, A cm^{-2}	$-Ip_{1/2}$, A cm^{-2}	$Ec_{1/2}$, V	$Ep_c - Ec_{1/2}$, mV
10	298	2.423×10^{-5}	2.420×10^{-5}	1.211×10^{-5}	0.2130	63.5
20		3.410×10^{-5}	3.419×10^{-5}	1.705×10^{-5}	0.2060	66.0
50		5.220×10^{-5}	5.266×10^{-5}	2.610×10^{-5}	0.1920	70.0
100		7.220×10^{-5}	7.208×10^{-5}	3.610×10^{-5}	0.1740	65.0
200		9.848×10^{-5}	9.784×10^{-5}	4.924×10^{-5}	0.1820	88.2
10	343	6.393×10^{-5}	6.930×10^{-5}	3.196×10^{-5}	0.2470	67.0
20		1.003×10^{-4}	9.650×10^{-5}	5.015×10^{-5}	0.2530	73.0
50		1.599×10^{-4}	1.633×10^{-4}	7.995×10^{-5}	0.2560	78.0
100		2.240×10^{-4}	2.250×10^{-4}	1.120×10^{-4}	0.2580	81.0
200		3.092×10^{-4}	3.132×10^{-4}	1.546×10^{-4}	0.2610	86.0
10	373	7.482×10^{-5}	8.460×10^{-5}	3.741×10^{-5}	0.3190	70.0
20		1.280×10^{-4}	1.259×10^{-4}	6.400×10^{-5}	0.3220	77.0
50		1.955×10^{-4}	1.917×10^{-4}	9.775×10^{-5}	0.3080	77.0
100		2.700×10^{-4}	2.750×10^{-4}	1.350×10^{-4}	0.3060	83.0
200		3.856×10^{-4}	3.806×10^{-4}	1.928×10^{-4}	0.3020	84.0
10	423	9.380×10^{-5}	1.020×10^{-4}	4.690×10^{-5}	0.3720	65.0
20		1.700×10^{-4}	1.680×10^{-4}	8.500×10^{-5}	0.3780	75.0
50		2.730×10^{-4}	2.690×10^{-4}	1.365×10^{-4}	0.3770	81.0
100		3.460×10^{-4}	3.340×10^{-4}	1.73×10^{-4}	0.3730	85.0
200		4.770×10^{-4}	4.700×10^{-4}	2.385×10^{-4}	0.3750	87.0

Such value is of the same order reported in recently literature for similar ILs [21] and it shows that they can dissolve an oxygen concentration approximately three times larger than in water. Moreover, it is also dimonstrated that the dissolved oxygen does not lower significantly with the increasing of temperature, at least up to 373 K [22].

One boundary condition regards the O_2 concentration, assumed to be zero at the IL solution–air interface. The other boundary is represented by the bottom of the cell, in which the condition of insulation imposes a null flux of oxygen. The employed cell has a thickness of liquid about 1 cm (l) and we can consider the simpler 'one-dimensional' diffusion problem. D_{O_2} is the diffusion coefficient of oxygen in the IL, takes as 1.5×10^{-10} m^2 s^{-1}, as reported in literature for similar liquids [23, 24].

In such conditions, the time necessary to reach the half of the initial oxygen concentration is estimated to be around 12 h. Thus, for every electrochemical experiment marked as in "purged solution", the employed ionic liquid was undergone to 12 h of nitrogen bubbling process.

Pt Wire Quasi-reference Electrode Stability

The Pt wire as quasi-RE was tested respect to the Ferrocene/Ferrocenium (Fc/Fc^+) redox couple (5 mM solution) in order to evaluate its stability in aerated and purged atmosphere of $EdMPNTf_2N$, also at high temperatures ranging from 343 up to 423 K. Several Cyclic Voltammetries (CVs) were conducted to evaluate the Pt wire potential shift with the increasing temperature. The CVs of ferrocene redox process were registered on platinum WE (50 mm^2) in the Teflon cell, resulting comparable to the curves reported in the literature for similar ILs, characterized by an almost reversible one-electron oxidation process.

In Table 1 are reported the data for purged atmosphere. Similar values are obtained for aerated solution of Ferrocene, whose stability in presence of oxygen was previously assessed [11] up to 22 h.

The diffusion coefficients for Ferrocene and Ferrocenium

$$i_p = 0.4463 \frac{F^{3/2}}{(RT)^{1/2}} n^{3/2} A D^{1/2} c v^{1/2},$$

were evaluated with the Randies–Sevcik equation assuming $A = 0.5$ cm^2, $c_{Fc\ or\ Fc^+} = 5 \times 10^{-6}$ mol cm^{-3} and $n = 1$.

The ratio between the diffusion coefficients of Fc and Fc^+ species, both determined plotting the peak current versus the scan rate square root, is close to unit within the temperature range considered. This implies that the half peak potential, $Ec_{1/2}$, can be reasonably used as the formal potential to scale the electrochemistry measurements in $EdMPNTf_2N$. Moreover the values of the diffusion coefficient (Table 2) are in the same range of other reported in literature for similar ILs [25]. In Fig. 2 are shown the CVs registered in purged atmosphere at 343 and 373 K. Plotting the $Ec_{1/2}$ versus the absolute temperature, the linear correspondence is maintained up to 423 K. Therefore, the shift in the potential of the quasi-reference of Pt electrode respect to the Fc/Fc^+ redox couple, within the range of temperature investigated, can be considered linear with the increasing absolute temperature (Fig. 3).

Table 2. Diffusion coefficients for the Ferrocene/Ferrocenium redox couple (5 mM) at several temperatures ranging from 298 up to 423 K

T, K	$Ec_{1/2average}$, V	D_{Fc^+}, cm^2 s^{-1}	D_{Fc}, cm s^{-1}
298	0.1930	9.97×10^{-8}	9.78×10^{-8}
343	0.2550	1.24×10^{-6}	1.24×10^{-6}
373	0.3110	9.41×10^{-6}	8.77×10^{-6}
423	0.3750	3.53×10^{-6}	3.27×10^{-6}

Table 3. Corrosion data regarding AISI 304 and AISI 1018 steels at 473 K in open air $EdMPNTf_2N$

Steels	OCV, V		I_{corr}, μA cm^{-2}	β_{an}, V dec^{-1}
	298 K	473 K		
AISI 304	–(0.51–0.54)	–(0.69–0.74)	4	155
AISI1018	–(0.72–0.75)	–(0.77–0.81)	6	240

Electrochemical Investigation on AISI 1018 Carbon Steel and AISI 304 Stainless Steel

Preliminary OCV registered at 473 K and in air conditions for the carbon steel and the stainless steel evidence a shorter time to reach plateau corrosion potential, around 3 h compared with the 9 h at room T [11].

The OCV values are more negative respect to the room temperature ones. The corrosion potential indicates the thermodynamic corrosion tendency of the material and it increases in magnitude with the temperature for both the alloys, though the corrosion potential for AISI 304 still shows a more resistant behavior respect to the carbon steel (see Table 3). Corrosion occurs due to oxygen, the formation of superoxide, O_2^- [26, 27] is already proved in aprotic solvents and it results stable in presence of water traces and in aerated condition.

The Tafel Plot extrapolations evidence that the stainless steel and the carbon steel show almost the same corrosion current densities, I_{corr}, that is 3–4 order of magnitude higher respect to the same at room temperature (Fig. 4). The mixed potential situation do not permit to estimate reliable corrosion rates values, but the kinetic of corrosion processes accelerates as the temperature rise.

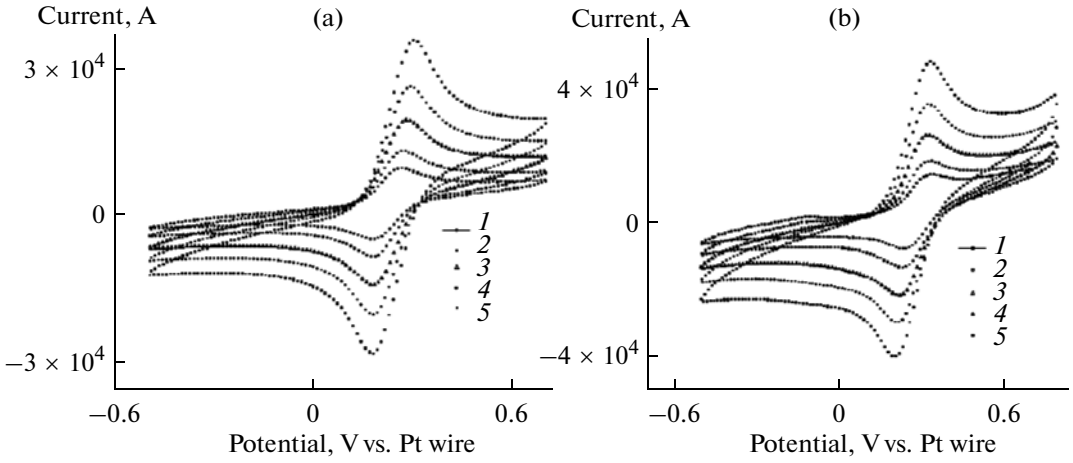

Fig. 2. Cyclic voltammetries of Fc/Fc^+ dissolved in $EdMPNTf_2N$ at 373 (a) and 343 K (b). Potential scan rate, mV/s: (*1*) 10, (*2*) 20, (*3*) 50, (*4*) 100, (*5*) 200.

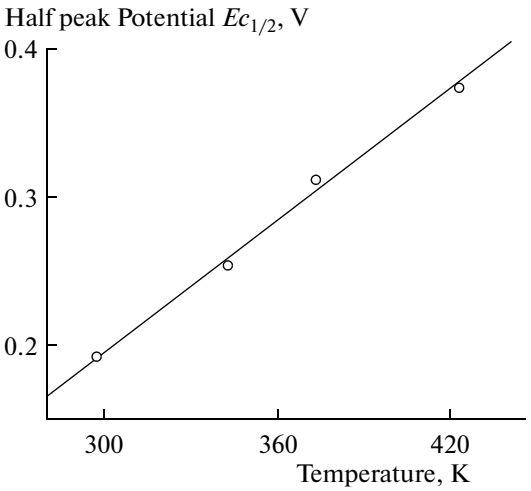

Fig. 3. Plot of the half peak potential of the redox couple Fc/Fc^+ versus temperature.

Electrochemical Investigation on Copper

As mentioned before, to shed some light on possible role of the dissolved oxygen as aggressive agent for the material in contact with the IL, WE decide to investigate the corrosion behavior of deaerated IL in contact with pure copper.

OCV measurements in purged atmosphere were conducted firstly de-aerating the liquid for 12 h with nitrogen at room temperature. The reactor was closed and the system heated up to the desired temperature. The OCV was registered until a quite stable (±5 K) temperature was reached. The time necessary to establish a stable open circuit potential was around 11 h. Every curve was independently registered using fresh copper samples and IL each time.

A better insight on the different behaviors of the metal is shown by the anodic Tafel plots: the Fig. 5 reports the plot for copper in disaerated (solid) ionic liquid solution and aerated ionic liquid (black circles) respectively at room and high temperature, up to 443 K. For copper purged solution the tendency to corrosion, indicated by the OCVs values, is significant lower (more positive potential) respect to the air condition, both at room and higher temperatures. Among the OCVs purged series, the curves registered at higher temperature (443 K) show a corrosion potential similar at which in aerated conditions and room temperature (Table 4).

Electrochemical Impedance Spectroscopy (EIS) Investigation on Copper

After the OCV curves and before the Tafel plot records, impedance spectra were conducted in the purged environment, applying an a.c. voltage of 5 mV in the frequency range from 65 kHz down to few mHz. The equivalent circuit employing in the simulation of the EIS spectra is in Fig. 6. It includes a Warburg (*W*)

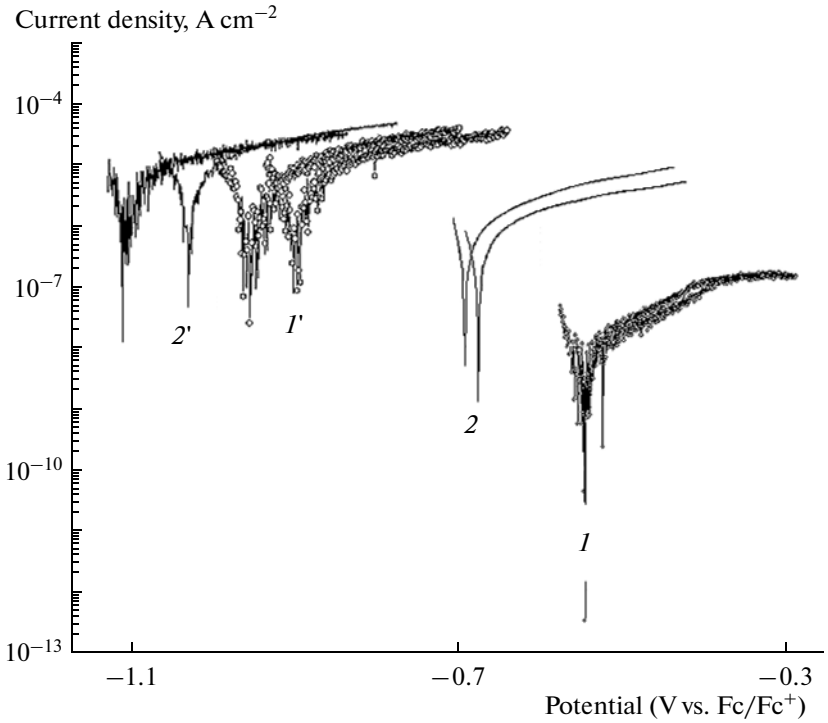

Fig. 4. Tafel plots on AISI 304 (*1*, *1*') and AISI 1018 (*2*, *2*') at 298 K (*1*, *2*) and 473 K (*1*', *2*') in aerated ionic liquid $EdMPNTf_2N$ (for each measurement, two curves are reported to test reproducibility).

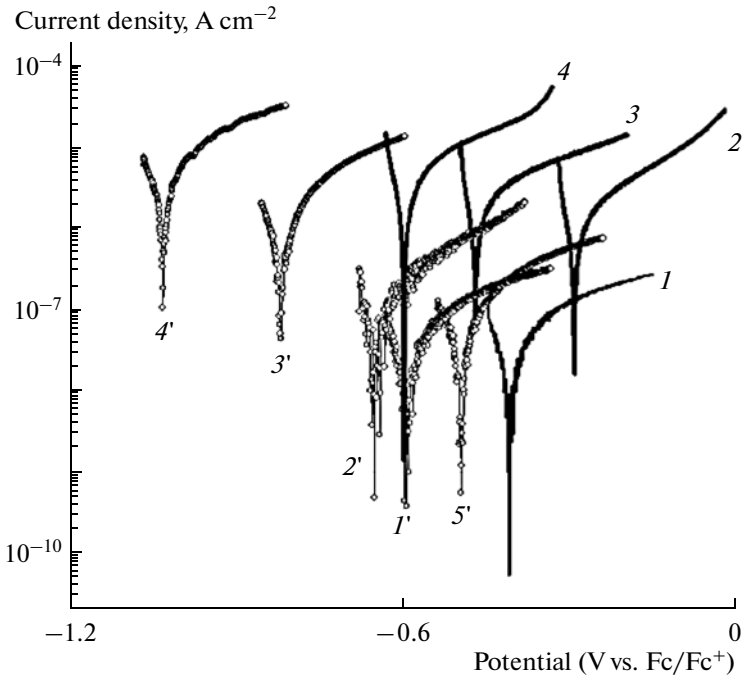

Fig. 5. Anodic Tafel Plots of copper in N_2 purged atmosphere (black bold lines) ionic liquid solution and aerated ionic liquid (black circles). Temperature, K: (*1*, *1*') 298, (*2*, *2*') 373, (*3*, *3*') 403, (*4*, *4*') 443, (*5*') 343.

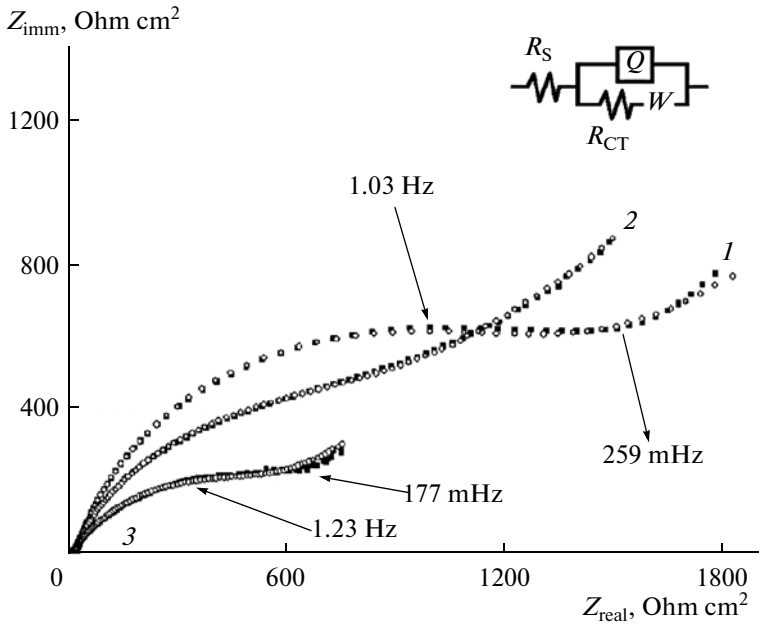

Fig. 6. Impedance spectra of the nitrogen purged solution of EdMPNTf$_2$N in contact with copper. Temperature in K: (*1*) 373, (*2*) 403, (*3*) 443.

element and the double layer capacitor is replaced by a constant phase element (*Q*). The simulated data are obtained by ZSimp Win 3.21 (Echem Software) and are reported in Table 5.

The Warburg diffusion is due to the diffusion of oxygen: at high frequency the value of the Warburg impedance is small, since diffusion reactants do not have to move very far. Whereas at low frequency, the

Table 4. Corrosion data regarding the Tafel curves reported in Fig. 5 for copper in aerated and N_2 purged of $EdMPNTf_2N$

Environment	Temperature, K	−OCV, V	I_{corr}, μA cm^{-2}	β_{an}, V dec^{-1}
N_2 purged	298	0.410	3.50×10^{-2}	0.271
	373	0.290	1.44	0.252
	403	0.460	2.38	0.314
	443	0.590	6.59	0.282
Air	298	0.615	6.90×10^{-2}	0.314
	343	0.510	1.70×10^{-1}	0.268
	373	0.635	5.20×10^{-1}	0.257
	403	0.800	2.60	0.270
	443	1.050	10	0.262

Table 5. EIS simulation parameters for copper-$EdMPNTf_2N$ system in N_2 purged atmosphere

Temperature, K	R_s, Ω cm^2	*Q-Yo*, S cm^{-2} s^n	*Q-n*	R_{CT}, Ω cm^2	σ, Ω cm^2 s$^{-1/2}$	D_{ox}, cm^2 s^{-1}
373	25.76	8.43×10^{-5}	0.83	1364	512	6.91×10^{-6}
403	14.14	1.25×10^{-4}	0.75	981	648	5.02×10^{-6}
443	9.29	2.8×10^{-4}	0.64	659	191	7.00×10^{-5}

reactants and the corrosion products have to diffuse further. The value of Warburg impedance (W) is given by [28]:

$$W = \frac{\sigma}{\sqrt{2\pi f}},$$

where σ is the Warburg coefficient, which is inversely proportional to the square root of the diffusion coefficient, as shown in the following equation [29]:

$$\sigma = \frac{RT}{n^2F^2\sqrt{2}Ac_{1/2}D_{ox}^{1/2}},$$

where R is the ideal gas constant (J K^{-1} mol^{-1}), T is the absolute temperature (K), $n = 1$ is the number of electrons involved in the superoxide formation, F is the Faraday constant (C mol^{-1}), $c_{1/2}$ is the oxygen concentration considered to be 3.5×10^{-7} mol cm^{-3} (an half respect c, concentration before N_2 purging), $A = 0.5$ cm^2 and D_{ox} is the diffusion coefficient (cm^2 s^{-1}) obtained from impedance measurements, reported in Table 5. D_{ox} remains in the range of 10^{-10} m^2 s^{-1} upto 403 K, the same order found in literature [23, 24, 27] for lower temperatures. Around 443 K, the diffusion coefficient rises up to 7.00×10^{-9} m^2 s^{-1} but further data on oxygen diffusion coefficients are not available in literature for the studied ionic liquid or similar in this range of temperatures. Moreover, the rising in temperature provokes the increasing conductivity of the ionic liquid (R_S) and the lowering of the charge transfer resistance (R_{CT}) value, confirming the favourable tendency of the corrosion process to occur.

The complex impedance plane plot consists mainly of the noticeably depressed semicircle at frequencies higher than 0.8 Hz, with the characteristic frequency, f_{max}, around 1 Hz, and of the so-called double-layer capacitance region at much lower frequencies ($f <$ 260 mHz). The found large time costant values, of the order of the seconds, are frequent in the slow diffusion processes occurring in corrosion phenomena. The semicircles are clearly visible in the plot at 373 and 443, while for the 403 K plot the semicircle and capacitance, or better CPE, region are overlaping. The CPE describes an ideal capacitor for $n = 1$ and an ideal resistor for $n = 0$. The intermediate values of n can describe a non homogeneous distribution of the molecular relaxation times in the electrolytes and/or a non uniform diffusion (a non uniform *RC* transmission lines) bulk processes. Up to 403 K, the electrode-material system shows a more capacitive behavior ($n =$ 0.84 at 373 K and 0.75 at 403 K) and, probably in this range of temperature, the CPE principally describes the non homogeneities in the double layer capacitance. Around the 443 K, the n value fall to 0.64, reasonably describing a situation of non homogenous

resistive behavior of the electrolytes, in which bulk diffusion processes are predominant.

CONCLUSIONS

The AISI 1018 and AISI 304 showed low corrosion current densities (4–6 μA cm^{-2}) in aerated ethyldimethyl-propylammonium bis(trifluoromethylsulphonyl)imide at 473 K. Apart from possible localized corrosion phenomena which still need to be assessed, such metal/ILs combination are potentially promising.

The framework changes when switching to copper. Here the aerated $EdMPNTf_2N$ provides current densities exceeding 10 μA cm^{-2} at 443 K. It worth mentioning that it lowers down to 6.6 μA cm^{-2} after N_2 purging at the same temperature. This fact confirms the importance of the dissolved oxygen in the corrosion processes for the copper. For copper substrates, further purging and drying processes of the ILs are highly advisable before the contact with the metal, to prevent copper corrosion.

ACKNOWLEDGMENTS

We gratefully acknowledge financial support provided by EC, Project FP6-2003-INCO-MPC2 (STREP) Contract Number: 015434, REACt, Self-sufficient Renewable Energy Air-Conditioning system for Mediterranean countries.

REFERENCES

1. Rogers, R.D. and Seddon, K.R., *Science 31*, 2003, vol. 302, p. 792.
2. Marsh, K.N., Deer, A., Wu, A.C.-T., Tran, E., and Klamt, A., *Korea. J. Chem. Eng.*, 2002, vol. 19, p. 357.
3. Blanchard, L.A., Hancu, D., Beckman, E.J., and Brennecke, J.F., *Nature*, 1999, vol. 399, p. 28
4. Holbrey, J.D. and Seddon, K.R., *Clean Prod. Proc.*, 1999, vol. 1, p. 223.
5. Welton, T., *Chem. Rev.*, 1999, vol. 99, p. 2071.
6. Endres, F., *ChemPhysChem*, 2002, vol. 3, p. 144.
7. Lin, Y.F. and Sun, I.W., *Electrochim. Acta*, 1999, vol. 44, p. 2771.
8. Takahashi, S., Koura, N., Kohara, S., Saboungi, M.L., and Curtiss, L.A., *Plasmas Ions*, 1999, vol. 2, p. 91.
9. Brennecke, J.F. and Magin, E.J., *AIChE J.*, 2001, vol. 47, p. 2384.
10. Balducci, A., Bardi, U., Caporali, S., Mastragostino, M., and Soavi, F., *Electrochem. Commun.*, 2004, vol. 6, p. 566.
11. Perissi, I., Bardi, U., Caporali, S., Fossati, A., and Lavacchi, A., *Sol. Energy Mater. Sol. Cells*, 2008, vol. 92, p. 510.
12. Zhang, Q. and Hua, Y., *Mater. Chem. Phys.*, 2010, vol. 119, p. 57.
13. Roosen, C., Müller, P., and Greiner, L., *Appl. Microbiol. Biotechnol.,* 2008, vol. 81, p. 607.
14. Bardi, U., Chenakin, S.P., Caporali, S., Lavacchi, A., Perissi, I., and Tolstoguzov, A., *Surf. Interface Anal.,* 2006, vol. 38, p. 1768.
15. Kosmulski, M., Gustafsson, J., and Rosenholm, J.B., *Thermochim. Acta*, 2004, vol. 412, p. 47.
16. Caporali, S., Lavacchi, A., Perissi, I., and Fossati, A., *Advances in Chemistry Research*, Vol. 6, Hauppauge, N.Y.: Nova Science Publishers, Inc., 2011, p. 315.
17. Buzzeo, M.C., Hardacre, C., and Compton, R.G., *Anal. Chem.,* 2004, vol. 76, p. 4583.
18. Anderson, J.L., Dixon, J.K., and Brennecke, J.F., *Acc. Chem. Res.*, 2007, vol. 40, p. 1208.
19. Seddon, K.R., Stark, A., and Torres, M., *Pure Appl. Chem.*, 2000, vol. 72, p. 2275.
20. Huddleston, J.G., Visser, A.E., Reichert, W.M., Willauer, H.D., Broker, G.A., and Rogers, R.D., *Green Chem.*, 2001, vol. 3, p. 156.
21. Anthony, J.L., Anderson, J.L., Maginn, E.J., and Brennecke, J.F., *J. Phys. Chem. B*, 2005, vol. 109, p. 6366.
22. Husson-Borg, P., Majer, V., and Costa Gomes, M.F., *J. Chem. Eng. Data,* 2003, vol. 48, p. 480.
23. Silvester, D.S., Rogers, E.I., Barrosse-Antle, L.E., Broder, T.L., and Compton, R.G., *J. Braz. Chem. Soc.*, 2008, vol. 19, p. 611.
24. Buzzeo, M.C., Klymenko, O.V., Wadhawan, J.D., Hardacre, C., Seddon, K.R., and Compton, R.G., *J. Phys. Chem. A*, 2003, vol. 107, p. 8872.
25. Brooks, C.A. and Doherty, A.P., *Electrochemistry Communications*, 2004, vol. 6, p. 6867.
26. Evans, R.G., Klymenko, O.V., Saddoughi, S.A., Hardacre, C., and Compton, R.G., *J. Phys. Chem. B*, 2004, vol. 108, p. 7878.
27. Huang, X., Rogers, E.I., Hardacre, C., and Compton, R.G., *J. Phys. Chem. B*, 2009, vol. 113, p. 8953.
28. Göhr, H., *Ber. Bunsen Ges. Phys. Chem.*, 1981, vol. 85, p. 274.
29. Dawson, J.L. and John, D.G., *J. Electroanal. Chem.*, 1980, vol. 110, p. 37.